

Community Structure and Function of Planktonic Crenarchaeota: Changes with Depth in the South China Sea

Anyi Hu · Nianzhi Jiao · Chuanlun L. Zhang

Received: 25 October 2010 / Accepted: 27 April 2011 / Published online: 20 May 2011
© Springer Science+Business Media, LLC 2011

Abstract Marine Crenarchaeota represent a widespread and abundant microbial group in marine ecosystems. Here, we investigated the abundance, diversity, and distribution of planktonic Crenarchaeota in the epi-, meso-, and bathypelagic zones at three stations in the South China Sea (SCS) by analysis of crenarchaeal 16S rRNA gene, ammonia monooxygenase gene *amoA* involved in ammonia oxidation, and biotin carboxylase gene *accA* putatively involved in archaeal CO₂ fixation. Quantitative PCR analyses indicated that crenarchaeal *amoA* and *accA* gene abundances varied similarly with archaeal and crenarchaeal 16S rRNA gene abundances at all stations, except that crenarchaeal *accA* genes were almost absent in the epipelagic zone. Ratios of the crenarchaeal *amoA* gene to 16S rRNA gene abundances decreased ~2.6 times from the epi- to bathypelagic zones, whereas the ratios of crenarchaeal *accA* gene to marine group I crenarchaeal 16S rRNA gene or to crenarchaeal *amoA* gene abundances increased

with depth, suggesting that the metabolism of Crenarchaeota may change from the epi- to meso- or bathypelagic zones. Denaturing gradient gel electrophoresis profiling of the 16S rRNA genes revealed depth partitioning in archaeal community structures. Clone libraries of crenarchaeal *amoA* and *accA* genes showed two clusters: the “shallow” cluster was exclusively derived from epipelagic water and the “deep” cluster was from meso- and/or bathypelagic waters, suggesting that niche partitioning may take place between the shallow and deep marine Crenarchaeota. Overall, our results show strong depth partitioning of crenarchaeal populations in the SCS and suggest a shift in their community structure and ecological function with increasing depth.

Introduction

The marine planktonic archaea, mainly constituted by mesophilic Crenarchaeota and Euryarchaeota, were first reported by Fuhrman et al. [23] and DeLong [18] using molecular DNA-based methods. Since then, extensive studies have demonstrated that these organisms are ubiquitous in the marine environments (e.g., [19, 24, 37, 40, 46]; also see review [58]). Because Crenarchaeota contribute substantially to prokaryotic abundance in the deep ocean [31, 37], they are expected to play an important role in biogeochemical cycling.

The discovery through metagenomic studies of marine [66] and soil [65] environments of crenarchaeal *amoA* genes was a significant breakthrough in our understanding of ecological function of mesophilic Crenarchaeota. Isolation of the first marine crenarchaeon *Nitrosopumilus maritimus* unambiguously demonstrated that it oxidizes

Electronic supplementary material The online version of this article (doi:10.1007/s00248-011-9866-z) contains supplementary material, which is available to authorized users.

A. Hu · N. Jiao (✉)
State Key Laboratory of Marine Environmental Science,
Xiamen University,
Xiamen 361005, People's Republic of China
e-mail: jiao@xmu.edu.cn

C. L. Zhang
State Key Laboratory of Marine Geology, Tongji University,
Shanghai 200092, People's Republic of China

C. L. Zhang
Department of Marine Sciences, University of Georgia,
Athens, GA 30602, USA

ammonia for energy production [35]. Previously, ammonia oxidation had been thought to be driven mainly by chemolithoautotrophic ammonia-oxidizing bacteria (AOB) [39, 53], which form two monophyletic lineages within the Beta- and Gammaproteobacteria, respectively. Now, a number of studies have shown that ammonia-oxidizing archaea (AOA) are widespread and more abundant than AOB in both marine and soil environments (e.g., [1, 6, 14, 16, 36, 42, 48, 70]), while some recent studies found that AOB play a more important role than AOA in N cycle in certain environments [15, 34, 45]. So far, putatively identified AOA include marine group I (MGI) [5, 50, 70], marine pSL12 [47], and HWCG III Crenarchaeota [17].

Some species of the marine Crenarchaeota may contribute to primary production through chemolithoautotrophic carbon fixation, especially in the dark oceans [2, 29, 31, 33]. Recently, a 3-hydroxypropionate-co-4-hydroxybutyrate autotrophic carbon fixation pathway was demonstrated in a thermoacidophilic crenarchaeon *Metallosphaera sedula* [8], and several key genes involved in this cycle were found in the mesophilic Crenarchaeon *N. maritimus* and *Cenarchaeum symbiosum* [20, 67], suggesting that this novel pathway may be important for archaeal CO₂ fixation in the ocean. Among these functional genes are *accA* and *accC* that code for the acetyl-CoA carboxylase, which have been used successfully for studying the CO₂ fixation by Crenarchaeota in freshwater lakes [3], marine sediments [52], and the open ocean [41, 72, 73].

Previous studies have shown that chemoautotrophic CO₂ fixation by marine microorganisms is an important microbial process providing fresh organic carbon in the dark ocean, while ammonia oxidation by Crenarchaeota might be an important, but not exclusive energy source for dark-ocean CO₂ fixation [31, 54]. However, only a few studies measured rates of dark CO₂ fixation in the ocean [31, 54, 71, 73], and there is little evidence about archaeal autotrophic CO₂ fixation at the gene level [41, 72, 73].

The South China Sea (SCS) is the world's largest marginal sea [11], which belongs to the "East Indies Triangle," where modern marine and terrestrial biodiversity reaches a global maximum [74]. However, little is known about the community structure and function of planktonic Crenarchaeota in the SCS. In this study, we analyzed the 16S rRNA, *amoA* and *accA* genes of archaea from three stations in the SCS. Our results show that the community structures of Crenarchaeota vary with depth at each station but change little horizontally at each depth zone among the three stations. Shifts of the crenarchaeal populations suggest changes in function with depth, with decreasing heterotrophic metabolism of Crenarchaeota in the meso- or bathypelagic zones, which is in contrast to what is observed in the North Atlantic Ocean [1] and Eastern Mediterranean Sea [16].

Materials and Methods

Sample Collection

Water samples were collected from three stations in the SCS during the GOE-1 cruise on board the RV "Dongfanghong" #2 between November 24 and December 20, 2006. Station S2 (18.78° N, 115.92° E) was located near the Southeast Asian Time-Series Station [69]; station Z97 (17.96° N, 118.97° E) was close to the Luzon Strait, within the winter upwelling area [61]; and station Y23 (11.51° N, 111.38° E) was located in the southwest of the SCS (Fig. 1). A Seabird SBE 9/17 plus CTD rosette sampler equipped with Go-Flo bottles was used to measure temperature and salinity, and to collect water samples. Concentrations of dissolved oxygen were determined immediately after sampling using the Winkler method [10].

Subsamples (2–3 L) were screened through 3- μ m pore-size polycarbonate filters (Millipore, Billerica, MA, USA) and free-living archaea were collected on 0.2- μ m pore-size polycarbonate filters (Millipore) at a pressure of <0.03 MP. The 3- μ m pore-size filters were considered to contain particle-associated populations of archaea, whereas the 0.2- μ m pore-size filters were considered to contain free-living populations of archaea [13]. Both types of filters were immediately frozen at -20°C on board the ship and during transportation and then stored at -80°C in the laboratory until further analysis.

DNA Extraction

DNA was extracted using the UltraClean Soil DNA kit (MoBio, San Diego, CA, USA) according to the manufacturer's instructions. DNA integrity and size were checked in a 0.8% agarose gel stained with SYBR Green I (Molecular Probes, Eugene, OR, USA), and the concentrations were quantified in duplicate by using FlexStation[®] 3 (Molecular Devices, Sunnyvale, CA, USA) with Quant-iT[™] dsDNA HS Assay Kit (Molecular Probes). A standard curve was generated using known amounts of Lambda DNA (Molecular Probes).

Quantitative PCR Analysis

Quantitative PCR (qPCR) was performed on an ABI PRISM 7500 system (Applied Biosystems, Foster City, CA, USA) with primers listed in Table 1. The abundances of the 16S rRNA genes of total archaea, MGI, and pSL12, the crenarchaeal *amoA* and *accA* genes, and the β -AOB *amoA* gene in all samples were determined in triplicate for each sample.

For 16S rRNA genes, the following reaction chemistry was used: 12.5 μ l of SYBR GreenER[™]-qPCR SuperMix

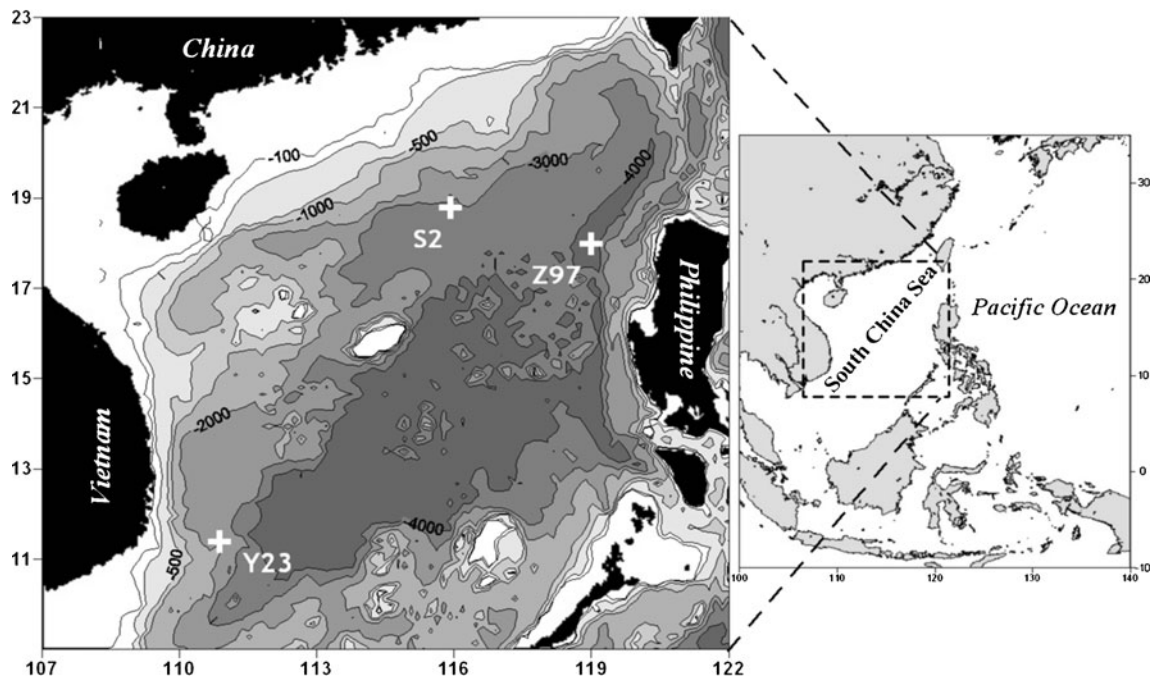


Figure 1 Location of the South China Sea and sampling stations

Universal (Molecular Probes), 50 nM ROX dye, 5 μ g BSA, 0.4 μ M of each primer and 1 μ l of template (1–10 ng) in a final volume of 25 μ l. Environmental clones SCS-MGI-A2 (GenBank accession no. GU252709) and SCS-pSL12-1 (GenBank accession no. GU252708) were served as standards (1.0×10^7 to 10^1 copies) for quantification of total archaea, MGI, and pSL12, respectively.

For functional genes, the 25 μ l reaction mixture contained 12.5 μ l of SYBR[®] Premix Ex Taq[™] (TakaRa, Dalian, China), 50 nM ROX dye, 5 μ g BSA, 0.4 μ M of each primer, 1 μ l template DNA of 1–10 ng. Standard curves were constructed for crenarchaeal *amoA* (1.1×10^7 to 11^1 copies) using a mixture of equal amounts of plasmid DNA extracted from a shallow clone S100_amoA_3

Table 1 Details of PCR primers used in this study

Target group	Primers	Sequence (5'-3')	Purpose	References
Archaea	21F	TTCCGGTTGATCCYGCCGGA	First round of archaeal 16S rRNA gene and nest PCR template DGGE analysis	[18]
	958R	YCCGGCGTTGAMTCCAAT		[18]
Archaea	rSAF-I ^a	CTAYGGGGCGCAGCAG	Second round of archaeal 16S rRNA gene and DGGE	[49]
	rSAF-II ^a	CTACGGGGCGCAGAGG		[49]
	Parch519R	TTACCGCGGCKGCTG		[51]
Archaea	Parch519F	CAGCMGCCCGGTAA	qPCR quantification of archaea	[51]
	Arc915R	GTGCTCCCCGCCAATTCCT		[62]
MGI	GI_751F	GTCTACCAGAACAYGTTC	qPCR quantification of MGI group	[47]
	GI_956R	HGGCGTTGACTCCAATTG		[47]
pSL12	pSL12_750F	GGTCCRCCAGAACGCGC	qPCR quantification of pSL12 group	[47]
	pSL12_876R	GTACTCCCCAGGCGGCAA		[47]
Crenarchaeal <i>accA</i> gene	Crena_529F	GCWATGACWGAYTTTGTYRTAATG	Cloning and qPCR quantification of crenarchaeal <i>accA</i> gene	[72]
	Crena_981R	TGGWTKRYTTGCAAYTATWCC		[72]
Crenarchaeal <i>amoA</i> gene	Arch-amoAF	STAATGGTCTGGCTTAGACG	Cloning and qPCR quantification of crenarchaeal <i>amoA</i> gene	[22]
	Arch-amoAR	GCGCCATCCATCTGTATGT		[22]
β -AOB <i>amoA</i> gene	amoA-1F	GGGGTTTCTACTGGTGGT	qPCR quantification of β -AOB <i>amoA</i> gene	[56]
	amoA-2R	CCCCTCKGSAAAGCCTTCTTC		[56]

a. A 40-bp-long pair GC clamp (CGCCCGCCGCGCGCGGGCGGGGCGGGGCACGGGGGC) was attached to the 5' end of the primers

(GenBank accession no. EU885983) and a deep clone S500_amoA_33 (GenBank accession no. EU885997), respectively, and for crenarchaeal *accA* (1.0×10^7 to 10^1 copies) using equal amounts of plasmid DNA extracted from a shallow clone S100_accA_3 (GenBank accession no. GQ507505) and a deep clone S500_accA_16 (GenBank accession no. GQ507545), respectively. Primers amoA-1F/amoA-2R [56] were used to determine the abundance of β -AOB *amoA* genes and clone Beta-AOB-D1 (GenBank accession no. GU252710) served as standards. The specificity of qPCR reactions was confirmed by melting curve analysis and agarose gel electrophoresis. The thermocycling parameters and efficiency of qPCR reactions are described in Table S1 in the Electronic Supplementary Materials (ESM).

DGGE Analysis

Denaturing gradient gel electrophoresis (DGGE) was performed using a Bio-Rad DCode Universal Mutation Detection System (Bio-Rad, Hercules, California, USA) according to the manufacturer's instructions. PCR products of archaeal 16S rRNA gene (rSaf-GC clamp/Parch519R) [49, 51] were applied on 8% (*w/v*) gels in $1 \times$ TAE buffer with a denaturing gradient of 30–55% denaturant (100% denaturing solution contains 40% formamide and 7 M urea). Electrophoresis was run at a constant temperature of 60°C and 75 V for 16 h. Gels were stained with SYBR Green I (Molecular Probes) for 30 min and rinsed in Mill-Q water for 30 min. The DGGE images were captured and analyzed using the GeneSnap and GeneTools software (SynGene-Synoptics, Cambridge, UK). DGGE bands were excised from DGGE gel and eluted with 50 μ l of sterile Mill-Q water for 24 h. PCR products were re-amplified using primers rSaf/Parch519R [49, 51], then purified, cloned and selected for sequencing.

PCR Amplification of Crenarchaeal Functional Genes and Construction of Clone Libraries

For the construction of clone libraries, crenarchaeal *amoA* gene was amplified with Arch-amoA primer pair [22] and crenarchaeal *accA* gene was amplified with Cren529F/Cren981R [72]. Cloning of PCR products was performed as described elsewhere [32]. Positive colonies were randomly selected, re-amplified using vector primers M-13F/M-13R, and sequenced using ABI 3730 XL sequencer (Applied Biosystems). Sequences reported in this work have been deposited in the GenBank database under accession numbers EU885956 to EU885973 (Archaeal 16S rRNA gene from DGGE bands), EU885974 to EU886195 (Crenarchaeal *amoA* gene), and GQ507495 to GQ507740 (Crenarchaeal *accA* gene).

Phylogenetic Analysis

Sequences of the archaeal 16S rRNA, *amoA*, and *accA* genes, along with the closest reference sequences retrieved from GenBank (<http://www.ncbi.nlm.nih.gov/>), were imported into ARB [44]. The sequences were aligned using ClustalW in ARB. Ambiguously aligned positions were corrected manually using the ARB-edit tool. The sequence bases frequency filters were used to exclude ambiguous positions and columns containing gaps. Bayesian trees were generated by the program MrBayes v.3.1.2 [55]. Five Markov chains in parallel were run with 5,000,000 generations and sampled every 100 generations (the first 7,500–10,000 “burn-in” trees were excluded from the consensus tree). Tree topologies were also evaluated with neighbor-joining and maximum-parsimony method using PAUP*4.0 [64].

Statistical Analysis

Operational taxonomic units (OTUs) were defined by using the furthest neighbor algorithm in DOTUR [59] using a cutoff of $\leq 5\%$ [5, 22, 32, 57]. Rarefaction, nonparametric richness estimators Chao1, and Shannon diversity index and Simpson's index were also calculated using DOTUR [59]. Coverage values were calculated using the following formula: $Coverage (C) = 1 - (n/N) \times 100$, where n is the number of clones that occurred only once, and N is the total number of clones analyzed [27]. The SONS software [60] was used to obtain an OTU distribution and to evaluate the percentage of OTUs shared between libraries.

Since normal distribution of the individual qPCR data was not always met, nonparametric Spearman's correlation analysis was used to test relationships among independent variables. Model II regressions with major axis were used to determine the slope of the relationship between paired variables using SMATR v.2.0 [21] because this method can estimate the line best describing the relationship between two independent bivariate data [68].

Results

Properties of Different Water Bodies

Vertical profiles of temperature, salinity, and dissolved oxygen were similar at stations S2 and Y23 (Fig. 2). The depth of halocline was around 100 m, and the depth of the potential thermocline was around 1,500 m at both stations; the depth of oxygen minimum zone was slightly higher at S2 (750 m) than at Y23 (900 m). The temperature profile at station Z97 was similar to S2 and Y23, but the halocline

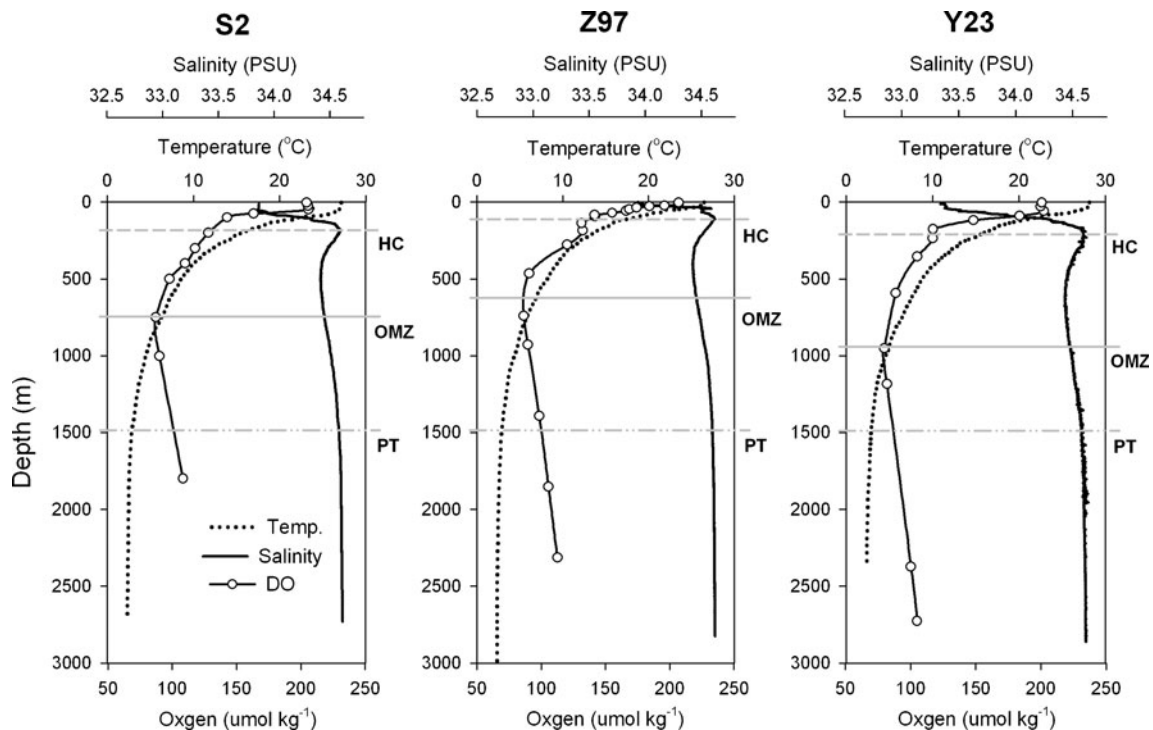


Figure 2 Depth profiles of hydrological properties (temperature, salinity, and dissolved oxygen) of sampling stations. *HC* halocline, *OMZ* oxygen minimum zone, *PT* potential thermocline

(<100 m) and oxygen minimum zone (~600 m) were shallower (Fig. 2).

Abundances of 16S rRNA, *amoA*, and *acca* Genes of Free-living Archaea

Gene abundances were quantified at three depths within each depth zone (epipelagic, <200 m; mesopelagic, 200–1,000 m; bathypelagic, >1,000 m) at stations S2 and Z97 (Fig. S1 in the ESM). Three samples were collected from the epi- and bathypelagic zones and two samples were collected from the mesopelagic zone at station Y23 (Fig. S1 in the ESM).

Archaeal, MGI, and pSL12 16S rRNA Genes

Depth profiles of the archaeal, MGI, and pSL12 16S rRNA gene abundances were similar at stations S2 and Y23. archaeal 16S rRNA gene abundance increased from near surface (5 m) values (1.25×10^3 copies ngDNA⁻¹ at station S2 and 1.58×10^3 copies ngDNA⁻¹ at station Y23) to the maximum value of 1.10×10^5 copies ngDNA⁻¹ at 75 m at station S2 or 9.22×10^4 copies ngDNA⁻¹ at 50 m at station Y23. 16S rRNA gene abundance then decreased with depth to about 1.20×10^4 copies ngDNA⁻¹ at 2,000 m at both stations (Fig. 3; Table S2 in the ESM). Depth profiles of MGI 16S rRNA gene abundance were similar to those of archaeal 16S rRNA genes and the abundance was of the same order as the archaeal 16S rRNA gene at similar depths

(Fig. 3). pSL12 16S rRNA gene abundance varied similarly to the MGI 16S rRNA but was one to three orders of magnitude lower than either MGI or archaeal 16S rRNA genes at the same depths (Fig. 3; Table S2 in the ESM).

At station Z97, gene abundances of archaeal, MGI, and pSL12 varied in the same range as those at stations S2 and Y23; however, the maximal values of archaeal and MGI gene abundances occurred at greater depth (~200 m) than at station S2 or Y23 (Fig. 3). Again, abundance of pSL12 16S rRNA genes was one to three orders of magnitude less than MGI or archaeal 16S rRNA gene abundances at the same depths (Fig. 3).

Overall, the average values of archaeal, MGI, and pSL12 16S rRNA gene abundances were greatest in the epi- or mesopelagic zones and lowest in the bathypelagic zone of the SCS (Table S2 in the ESM).

amoA- and *acca* Genes

Similar to the general patterns of the archaeal- or MGI 16S rRNA genes, the abundance of crenarchaeal *amoA* genes was low near the surface then increased with depth to maximal values at the base of the epipelagic zone or in the mesopelagic zone, and decreased again to the bottom water (Fig. 3). At stations Z97 and Y23, the maximal values of crenarchaeal *amoA* gene abundance occurred at the same depths as maxima for archaeal or MGI 16S rRNA genes, respectively, whereas it occurred at a greater depth (200 m)

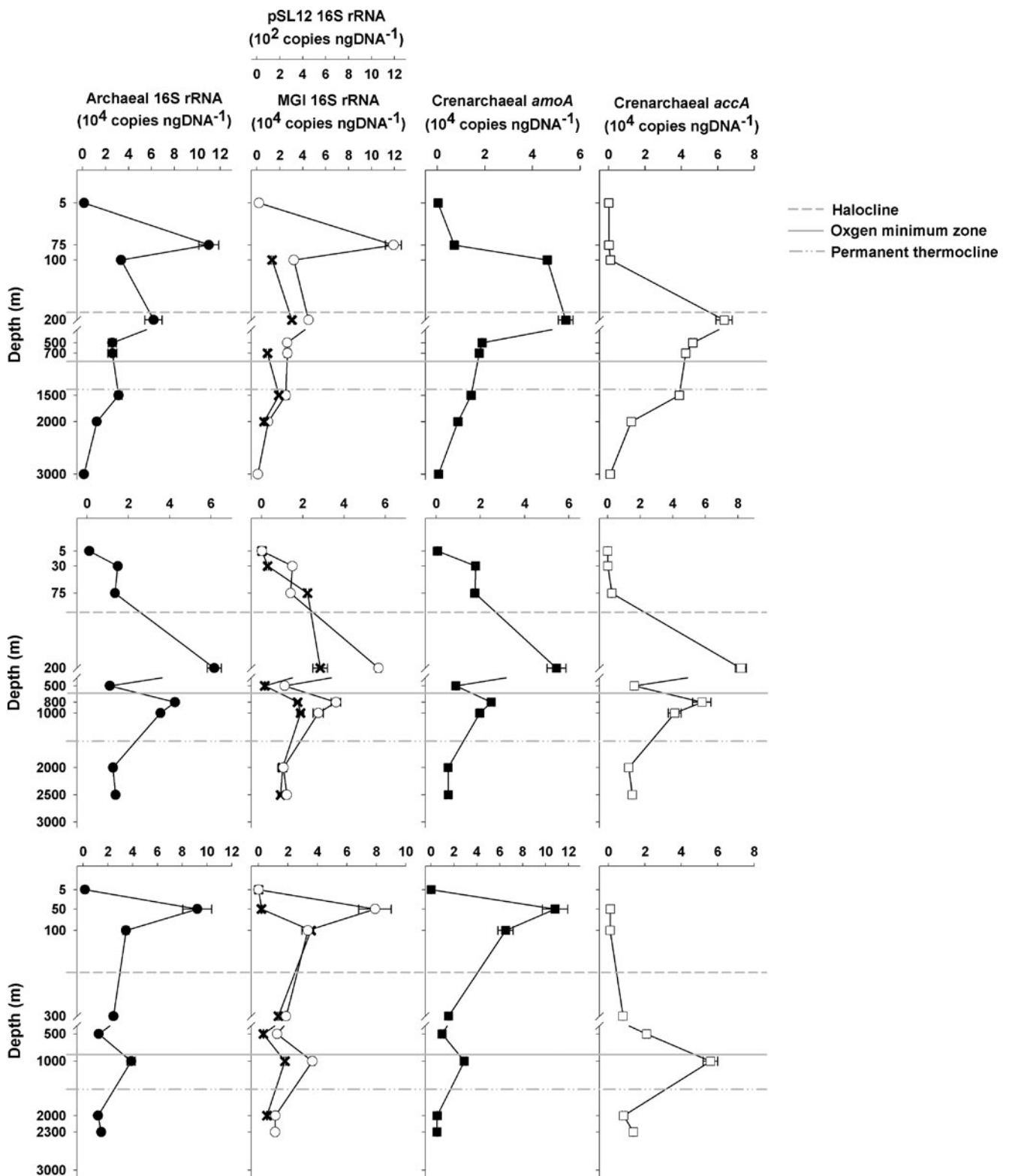


Figure 3 Vertical profiles of abundance of archaea, MGI, and pSL12 16S rRNA genes and crenarchaeal *amoA* and *accA* genes measured by qPCR at stations S2, Z97 and Y23. Bars denote one standard error of

the triplicate qPCR determination and are not visible when less than the width of the data point. All samples contained free-living organisms

than the maxima for archaeal or MGI 16S rRNA genes at station S2 (Fig. 3). Archaeal *accA* gene abundance varied

similarly with the *amoA* gene abundance at stations S2 and Z97, with maxima at the same depths; however, the profile

was dramatically different at station Y23, where the maximal value occurred at much greater depth (1,000 m) (Fig. 3).

Overall, the average abundance of the *amoA* gene was greatest in the epipelagic zone and lowest in the bathypelagic zone (Table S2 in the ESM). For the crenarchaeal *accA* gene, the average abundance was highest in the mesopelagic zone and lowest in the epipelagic zone (Table S2 in the ESM).

Correlations among Different Gene Abundances (16S rRNA, *amoA*, and *accA*) of Free-living Archaea

The ratio (slope) of crenarchaeal *amoA* gene abundance versus 16S rRNA gene abundance (sum of MGI and pSL12) decreased with depth from 1.45 for the epipelagic zone to 1.15 for the mesopelagic zone, and to 0.56 for the bathypelagic zone (Fig. 4a). We excluded the 5 and 75 m samples from station S2 because of the large uncertainty associated with the extremely low values of *amoA*/16S gene ratio.

The ratio of crenarchaeal *accA* gene to MGI 16S rRNA gene was also extremely small in the epipelagic zone (slope=-0.002) and should be interpreted with caution. However, the ratio was high in the mesopelagic zone (slope=1.65) and the bathypelagic zone (slope=1.67) (Fig. 4b). The ratio between the *accA* gene and the *amoA* gene increased from the epipelagic zone (slope=0.007) to the bathypelagic zone (slope=2.95) (Fig. 4c).

We found statistically significant correlations between *amoA* gene and crenarchaeal 16S rRNA gene abundances for the epipelagic (Spearman's correlation: $r=0.733$, $p<0.01$, $n=8$) and the mesopelagic ($r=0.988$, $p<0.001$, $n=10$) zones but not for the bathypelagic zone ($p=0.148$). The correlation between *accA* gene and the MGI 16S rRNA gene was statistically significant for the mesopelagic zone (Spearman's correlation: $r=0.9$, $p<0.001$, $n=10$) and the bathypelagic zone ($r=0.79$, $p<0.05$, $n=7$) but not for the epipelagic zone ($p=0.419$). A statistically significant correlation between crenarchaeal *accA* and *amoA* genes was only found for samples from the mesopelagic zone (Spearman's correlation: $r=0.92$, $p<0.001$, $n=10$).

Abundance of Free-living AOB

The abundance of β -AOB *amoA* genes was determined in order to provide comparison with the archaeal *amoA* genes. Overall, the β -AOB *amoA* genes were only detected in seven out of 26 samples. Among the seven positive samples, the ratios of AOA to β -AOB *amoA* copy number ranged from 2 to 1,000 except for the 5 m sample at station Y23, which had slightly more β -AOB *amoA* genes than AOA (AOA/AOB ratio= ~ 0.8) (Table S2 in the ESM).

Abundance of 16S rRNA Genes of Particle-Attached Archaea

The abundance of particle-associated ($>3 \mu\text{m}$) archaeal 16S rRNA genes from station Y23 were measured in three samples (100, 500, 2,000 m) to determine whether pre-filtration removed a significant fraction of total archaeal community in the SCS (Table S3 in the ESM). The ratio of particle-associated archaeal 16S rRNA gene to free-living archaeal 16S rRNA gene abundance ranged from $\sim 1\%$ in the 100 m sample to $\sim 7\%$ in the 2,000 m, suggesting that particle-associated archaea contributed a minor portion to total archaea in the SCS.

DGGE analysis of Archaeal Communities in Epi-, Meso- and Bathypelagic Zones

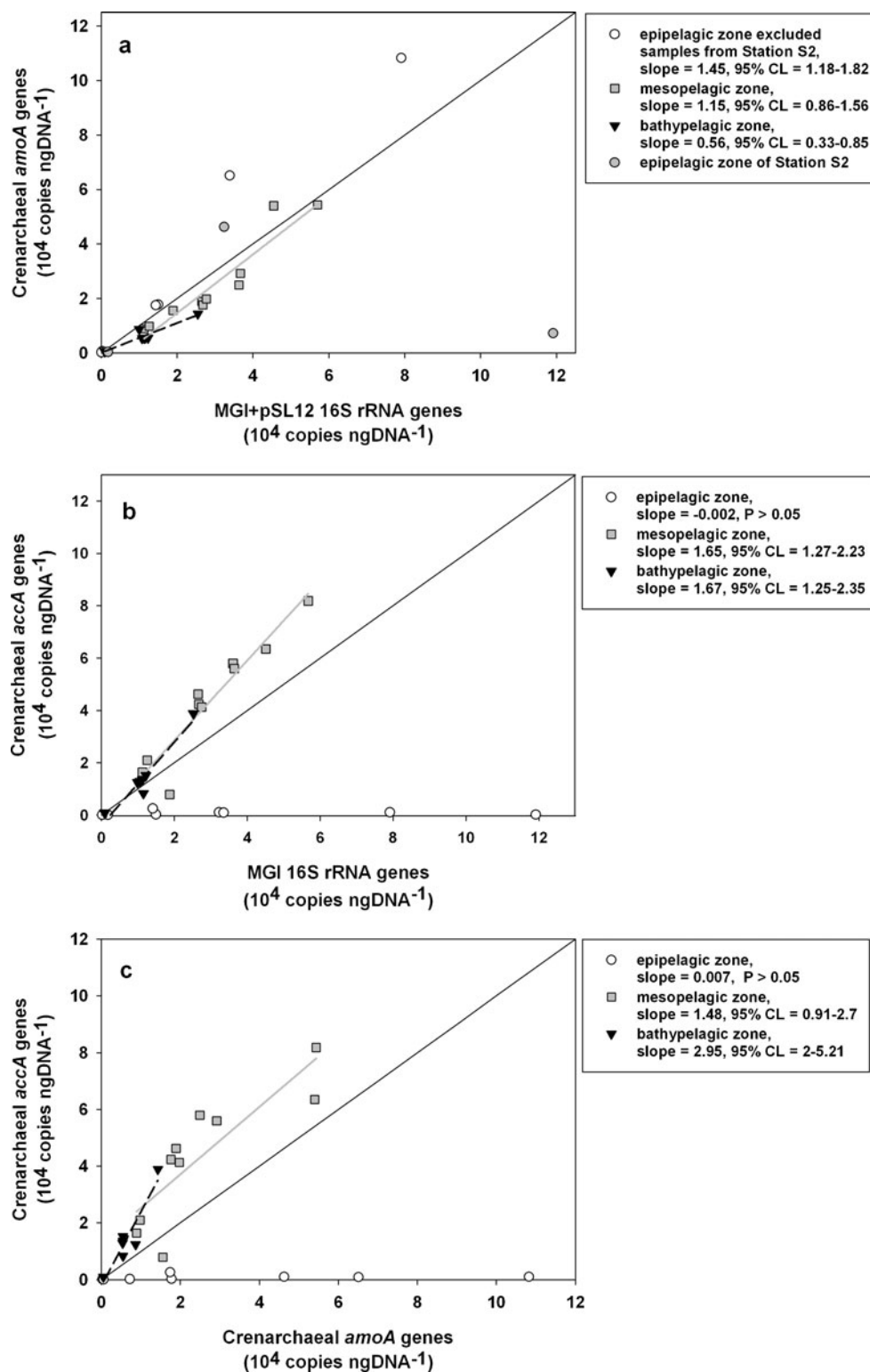
Archaeal community structures were evaluated by DGGE analysis of 16S rRNA gene fragments. Three samples from each station were chosen as representatives of the free-living archaea from the epi- (100 m except at station Z97, which was 75 m), meso- (500 m), and bathypelagic (2,000 m) zones (Fig. S1 in the ESM); furthermore, particle-attached archaea were evaluated for station Y23 for all three depth zones.

DGGE bands from epipelagic zone samples were distinct from those of the meso- or bathypelagic zones (Fig. 5), indicating changes in the community structures of archaea with increasing depth. In contrast, DGGE profiles in water masses of equivalent depths were similar to each other among the three stations (Fig. 5).

The DGGE profiles of particle-associated samples obtained from station Y23 were also different with depth (Fig. 5); however, samples at meso- or bathypelagic depths were similar to DGGE patterns of the free-living samples in the epi- or mesopelagic depths. For example, Y500m ($3 \mu\text{m}$) and Y100m ($0.2 \mu\text{m}$) shared several bands, while Y2000m ($3 \mu\text{m}$) exhibited a similar DGGE pattern as Y500m ($0.2 \mu\text{m}$) rather than with Y2000m ($0.2 \mu\text{m}$) (Fig. 5). The relative proportions of particle-associated archaeal 16S rRNA genes increased with depth (Table S3 in the ESM), implying that particle-associated archaea at depth may be derived from free-living archaea attached to particles falling from shallower depth.

In total, 18 DGGE bands with unique melting positions in the gel were excised and sequenced. Most of them clustered with the MGI lineage, which could be further divided into three subclades: MGI- α , MGI- β , and MGI- γ , except that one band recovered from particle-associated sample Y23_500m was related to sequences of the marine Euryarchaeota marine group III (Fig. 6). These results suggest the dominance of MGI in archaeal communities, which is consistent with the qPCR data presented above. Furthermore, the pattern of the

Figure 4 Ratios of crenar *amoA* versus 16S rRNA genes (sum of MGI and pSL12) (a), crenarchaeal *accA* versus MGI 16S rRNA genes (b), and crenarchaeal *accA* versus *amoA* genes (c) in samples from the SCS. The pSL12 gene abundance is not added to MGI 16S rRNA gene when drawing correlation with *accA* genes because it is unknown whether the pSL12 group contains any *accA* genes. Samples from different water masses are indicated by different symbols: circles (white or gray), epipelagic zone samples; squares (gray), mesopelagic zone samples; and triangles (black), bathypelagic zone samples. Regression lines, slopes of model II regression are shown: solid line (gray), mesopelagic zone samples; dashed line (black), bathypelagic zone samples; diagonal lines indicate a 1:1 relationship; 95% confidence limits of slope are also shown when regression is statistically significant ($p < 0.05$)



DGGE and the 16S rRNA gene sequences retrieved from the gels collectively indicate that MGI- α and MGI- β occurred in the epipelagic zone (six of seven band sequences), while the MGI- γ dominantly occurred in the bathypelagic zone (eight of ten band sequences) (Fig. 6).

Clone Libraries of *amoA* and *accA* Genes of Free-living Archaea

A total of 222 *amoA* sequences and 245 *accA* sequences were obtained from our samples (Table 2). These contained 41 unique operational taxonomic units (OTUs) of cren-

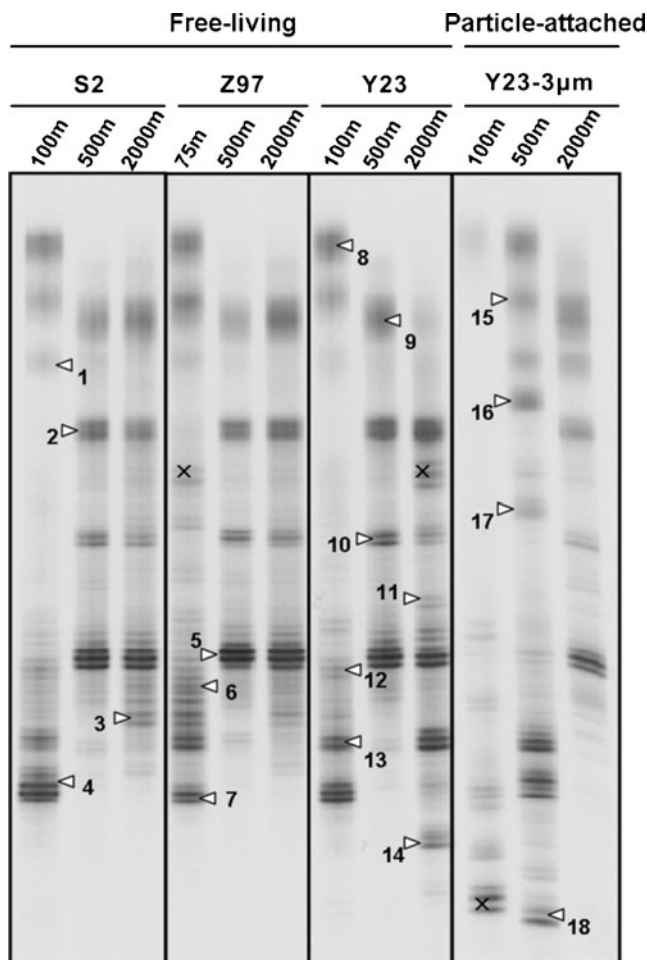


Figure 5 DGGE pattern of archaeal 16S rRNA genes from free-living and particle-attached populations collected from different depths at the three stations (S2, Z97 and Y23). The numbered bands were excised and sequenced. *Error marks* indicate a smeary band or a band not sequenced

archaeal *amoA* genes and 41 OTUs of crenarchaeal *accA* genes based on 5% distance cutoff at the DNA level. The number of OTUs per sample varied between five and 13 for *amoA* genes and between five and nine for *accA* genes (Table 2). These clone libraries should represent the diversity of crenarchaeal *amoA* and *accA* genes in the SCS, as indicated by high coverage values (Table 2). Moreover, the number of observed crenarchaeal *amoA* and *accA* OTUs, on average, represented 77% and 74% of the total number of AOA predicted (Chao1) to occur at each depth, respectively (Table 2).

For both genes, phylogenetic analyses showed two major clusters, namely the “shallow group” and “deep group”. The “shallow group” contained sequences almost exclusively derived from epipelagic water and the “deep group” contained sequences mostly from the meso-/bathypelagic waters (Figs. 7 and 8). The depth stratification was also supported by the OTU analysis using SONS software [60] (Table 3). This depth distribution correlates with the

distribution of archaeal 16S rRNA DGGE analysis, which collectively indicate a high level of congruence between *amoA* and *accA* genes at different depths. Although precise correlation between the two types of genes could not be determined due to the lack of reference species in culture, similar shifts in the relative abundance of specific phylotypes for each gene in vertical profiles suggest that specific organisms are represented by the corresponding 16S rRNA, *amoA*, and *accA* genes. For instance, genes in the *amoA/accA* shallow group I were the most abundant phylotypes in the epipelagic layer; whereas *amoA* deep group I/*accA* deep group III, and *amoA* deep group IV/*accA* deep group I had similar distributions in the meso- and bathypelagic zones (Fig. 8).

Discussion

Variation in Ecological Function of Crenarchaeota at Different Depths

Our qPCR data indicate that a slightly decreasing trend in gene abundance ratios of crenarchaeal *amoA* to 16S rRNA (sum of MGI and pSL12) with increasing depth, with the highest ratio occurring in the epipelagic samples and the lowest ratio in the bathypelagic samples. The crenarchaeal *amoA* to 16S rRNA ratios (0.56–1.45) reported here are close to previously published estimates from various oceanic areas including the Pacific Ocean [6, 7, 12, 47, 57], North Sea [30, 70], Tyrrhenian Sea [72, 73], and Arctic Ocean [36], indicating that most Crenarchaeota have the ability to perform ammonia oxidation in the SCS. In contrast, two recent studies have shown that the bathypelagic Crenarchaeota in the North Atlantic and Eastern Mediterranean Sea are lack of the *amoA* gene (ratios of *amoA* to 16S rRNA, <0.05), suggesting that bathypelagic Crenarchaeota in these regimes likely use organic substrates as carbon and energy sources rather than performing autotrophy [1, 16]. A similar water-mass dependent shift in *amoA*/MGI 16S rRNA gene ratio is reported in Antarctic water [36], which has the lowest ratios in the lower epipelagic zone. In the present study, however, the ratio of crenarchaeal *amoA* to 16S rRNA gene in the bathypelagic zones (~ 0.56) of the SCS is much higher than those ($<10^{-1}$) of the North Atlantic Ocean [1] and East Mediterranean Sea [16]. On the other hand, a metagenomic study of the North Pacific Subtropical Gyre shows that most if not all crenarchaeal cells at a depth of 4,000 m in the North Pacific Subtropical Gyre contain genes associated with ammonia oxidation [38]. Recent studies suggest that this discrepancy may be due to the failure of quantitative PCR primers to amplify the *amoA* genes of some deep-sea Crenarchaeota [12, 38, 73].

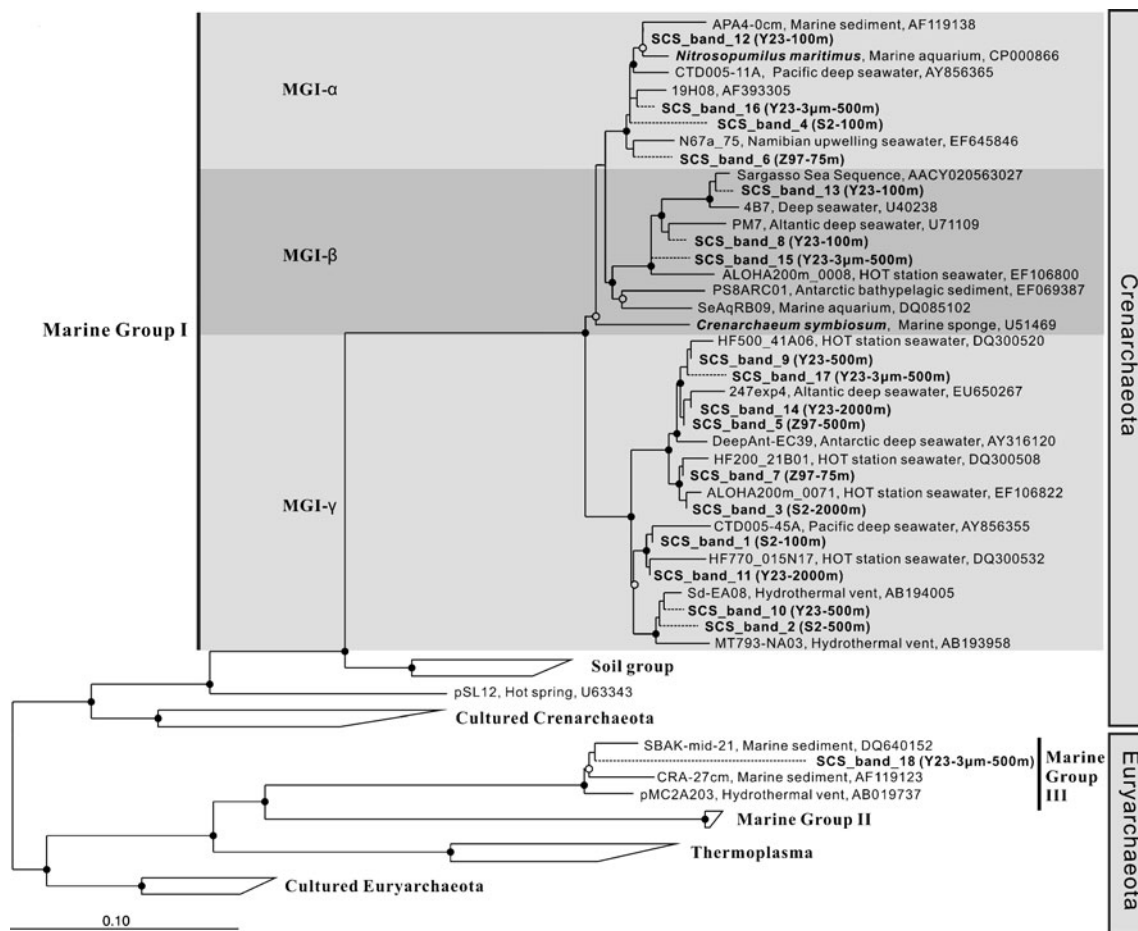


Figure 6 Phylogenetic tree of archaeal 16S rRNA genes from free-living and particle-attached populations of archaea. The tree was initially constructed based on nearly full-length (>1,200 bp) sequences using Bayesian analysis in combination with filters excluding highly variable positions. Partial sequences from DGGE bands in this study are in bold and indicated by *dashed lines* of tree branches; these sequences were inserted into the tree using the parsimony interactive

tool in ARB, without affecting the overall tree topology. The numbers for DGGE bands on the tree correspond to the numbered bands in Fig. 5. *Solid circles* (posterior probability values of >80%) and *open circles* (posterior probability values of >50%) indicate nodes supported by Bayesian analysis. Nodes without circles were not resolved. *Scale bar* indicates 0.1 nucleotide substitution per site

Table 2 Diversity indices of free-living crenarchaeal *amoA* and *accA* clone libraries from the SCS

Crenarchaeal <i>amoA</i>						Crenarchaeal <i>accA</i>				
Samples	<i>n</i>	No. of OTUs ^a	C (%)	H'	Chao1	<i>n</i>	No. of OTUs	C (%)	H'	Chao1
S2_100m	21	5	90.5	1.18	6	26	9	76.9	1.52	17
S2_500m	26	8	80.8	1.51	13	30	8	83.3	1.18	11
S2_2000m	26	12	76.9	2.30	17	30	9	83.3	1.66	12
Z97_75m	30	11	86.7	2.20	13	28	9	85.7	1.84	11
Z97_500m	26	10	76.0	1.90	18	29	8	79.3	1.19	23
Z97_2000m	23	8	82.6	1.79	11	25	6	96	1.64	6
Y23_100m	22	6	95.5	1.64	6	26	9	84.6	1.86	11
Y23_500m	25	13	68.0	2.29	20	28	7	85.7	1.28	10
Y23_2000m	23	7	95.7	1.60	7	24	5	100	1.52	5

n number of clones sequenced, *C* coverage

^aOTUs were defined as 5% divergence at the DNA level

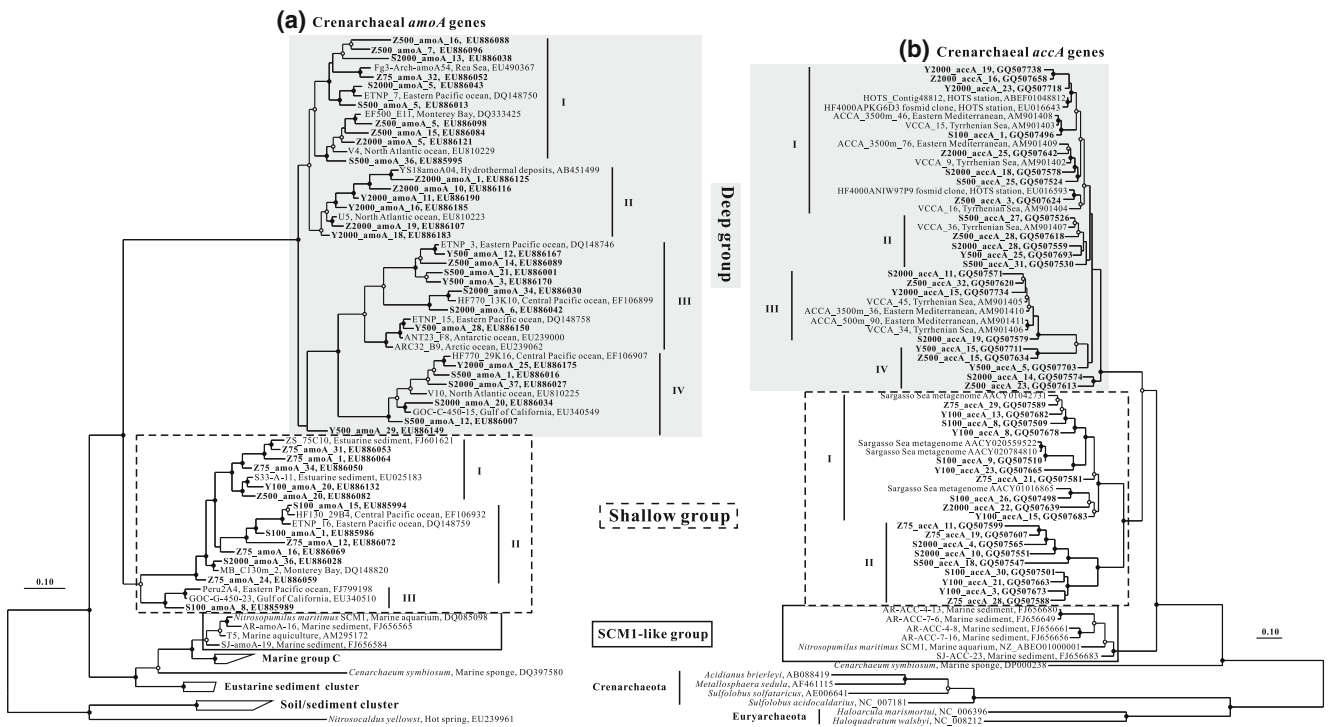


Figure 7 Phylogenetic trees of crenarchaeal *amoA* (a) and *accA* genes (b) from free-living organisms. The tree was constructed with reference sequences using Bayesian methods. Sequences with $\leq 5\%$ distance cutoff were represented by one of them. Clone sequences recovered in this study are in boldface. Sequences in shades or outlined by the dashed lines between crenarchaeal *amoA* and *accA*

trees represents putative common lineages of the genes. *Solid circles* (posterior probability values of $>80\%$) and *open circles* (posterior probability values of $>50\%$) indicate nodes supported by Bayesian analysis. Nodes without circles were not resolved. *Scale bar* indicates 0.1 nucleotide substitution per site

On the other hand, checking against qPCR results we find the highest ratios of crenarchaeal *accA* to *amoA* gene and crenarchaeal *accA* to 16S rRNA gene in the bathypelagic zone (Fig. 4b, c), which raises the possibility that the

ecological function of Crenarchaeota changes across the water depth zones: Crenarchaeota in epipelagic zone may grow chemoorganoheterotrophically, while in meso- and bathypelagic waters, most Crenarchaeota could fix CO_2 as a

Figure 8 Depth distribution of phylogenetic community structures of crenarchaeal *amoA* (a) and *accA* genes (b) recovered from free-living organisms from the SCS. The relative abundance of each phylotype in the clone library named in Fig. 7 was calculated and represented in a column diagram. The asterisks indicate sample collected from the 75-m depth at station Z97

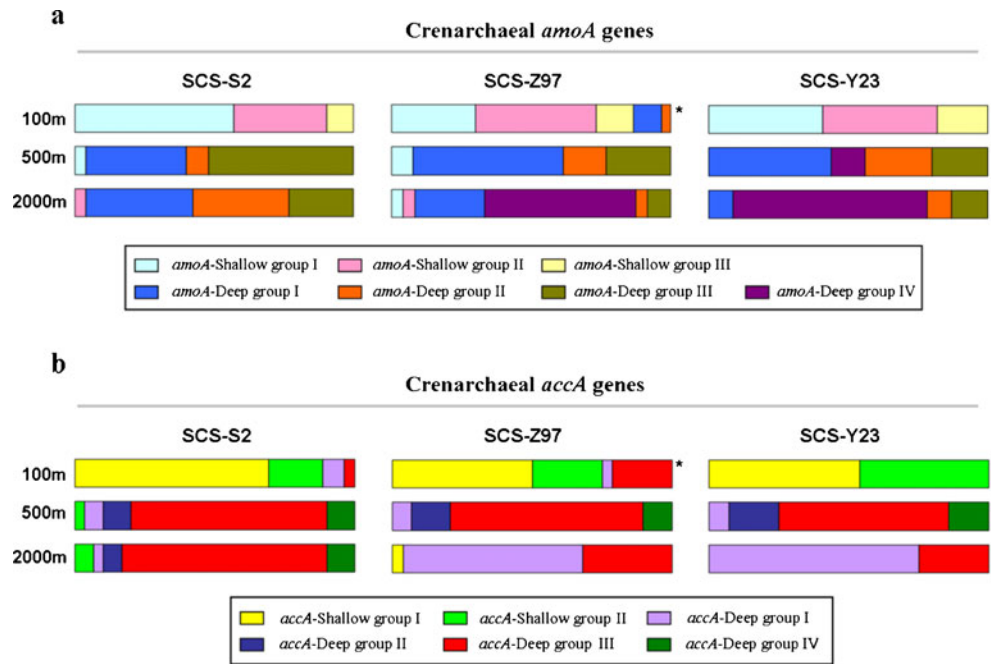


Table 3 Abundance-based Sørensen-type (L_{abd}) similarities among crenarchaeal *amoA* (below the diagonal) and *accA* (above the diagonal) clone libraries

Clone library	S2_100m	S2_500m	S2_2000m	Z97_75m	Z97_500m	Z97_2000m	Y23_100m	Y23_500m	Y23_2000m
S2_100m	–	0.07	0.07	0.79	0.07	0.07	0.80	0.07	0.07
S2_500m	0.00	–	0.77	0.35	1.00	0.69	0.00	1.00	0.32
S2_2000m	0.06	0.64	–	0.35	0.76	0.36	0.00	0.83	0.27
Z97_75m	0.82	0.05	0.36	–	0.35	0.17	0.56	0.00	0.17
Z97_500m	0.07	0.69	0.47	0.07	–	0.68	0.00	1.00	0.75
Z97_2000m	0.00	0.38	0.18	0.06	0.33	–	0.00	0.52	0.89
Y23_100m	0.94	0.06	0.06	0.98	0.07	0.07	–	0.00	0.00
Y23_500m	0.00	0.92	0.76	0.14	0.68	0.65	0.00	–	0.47
Y23_2000m	0.00	0.20	0.11	0.00	0.14	0.95	0.00	0.78	–

Values of L_{abd} greater than or equal to 0.5 are set in bold

carbon source. Our results are consistent with a previous report employing MICRO-CARD-FISH method that shows decreasing heterotrophic activity of Crenarchaeota in the meso- or bathypelagic zones of the SCS [75]. However, Hallam et al. [28] retrieve six *amoA* and four *accA* genes from the Sargasso Sea metagenomic dataset (surface water sample), indicating a ratio of *accA/amoA* gene copy number close to 1:1. Given that the primers used here were designed based on a few available sequences [72], it is possible that some *accA* genes of epipelagic Crenarchaeota may be missed in our qPCR assays. Therefore, further studies, including quantification of other genes and metagenomic and proteomic approaches, are needed to shed light on the modes of carbon metabolism of epipelagic Crenarchaeota.

Dark CO₂ fixation by microbial processes proves to contribute substantially to the organic carbon demand of microbial food web in the meso- and bathypelagic zones [54], although the energy source is still unclear. Consistent with previous studies [41, 72], we found most Crenarchaeota in deep waters of the SCS harbor *accA* genes, providing crucial evidence that autotrophic Crenarchaeota play an important role in dark CO₂ fixation. This conclusion is also supported by recent multiphase analyses of marine Crenarchaeota by Yakimov et al. [73]. Combining H¹⁴CO₃ in situ incubation with proteomics analyses, these authors show that bathypelagic Crenarchaeota at a depth of 3,480 m in the Central Mediterranean Sea are actively involved in dark CO₂ fixation [73].

Adaptability of Marine Crenarchaeota

Planktonic archaeal communities seem to be rather similar spatially on the horizontal scale [43, 46], except where different water masses meet [1, 25, 36]. This is further supported by our observation that similar crenarchaeal communities occur in the same depth zone among three

stations in the SCS. Vertically, however, two distinct populations (“shallow group” and “deep group”) occupy the epi- and meso-/bathypelagic waters in the SCS, respectively. The slow water exchange between the SCS and the water masses surrounding it [69] may facilitate the uniform horizontal distribution and vertical stratification of crenarchaeal populations (Fig. 7 and Table 3). The predominance of MGI- α and MGI- β groups in shallow water, and the predominance of MGI- γ in deep water have been observed in various oceanic regions [4, 43, 46]. A similar depth-specific phylogeny within marine Crenarchaeota is also observed based on analysis of internal transcribed spacer sequences [26]. Our results suggest coherent phylogenies among crenarchaeal 16S rRNA, *amoA*, and *accA* genes that are defined by water stratification in the SCS. These results may indicate niche adaptation for different crenarchaeal populations in different water bodies in the ocean [73].

Mesophilic Crenarchaeota is proposed to form a new archaeal phylum—Thaumarchaeota, which may have originated from hyperthermophilic Crenarchaeota, although the time of radiation is still unclear [9, 63]. During their long evolutionary history, marine Crenarchaeota may have adapted to various aquatic environments and become distributed from the ultra-oligotrophic open ocean to the eutrophic coastal oceans and from surface oceans to aphotic deep oceans. Our data, corroborating with previous data from various oceanic regions, demonstrate the existence of the depth-related separation of marine Crenarchaeota [6, 57, 73]. Mincer et al. [47] propose that the niche partitioning of AOA may be due to photoinhibition-resistance adaptations. We agree that the light may be a critical factor causing the depth-related separation as we have observed that marine Crenarchaeota may divide into two groups near the base of the euphotic zone (Hu and Jiao, unpublished data). However, it is unclear how light or other environmental factors may affect this depth partitioning [57].

In summary, our study demonstrates the depth partitioning of marine Crenarchaeota; whereas, horizontally the archaeal populations show homogeneous distribution in the SCS. The ratio of crenarchaeal *amoA*/16S rRNA gene abundances slightly declines with depth, while ratios of crenarchaeal *accA*/MGI 16S rRNA gene abundances and crenarchaeal *accA/amoA* gene abundances increase with depth. These results suggest that the ecological roles of marine Crenarchaeota may change with depth in the SCS: a great fraction of Crenarchaeota in the epipelagic waters may grow chemoorganoheterotrophically, while in meso- and bathypelagic waters, most Crenarchaeota could fix CO₂ as a carbon source.

Acknowledgments We thank the captain and crew of the RV “Dongfanghong” #2, L. Wang and R. Zong for assistance in collecting the samples, Z. Y. Sun and J. Zhu for providing the temperature and salinity data, and M. H. Dai for providing the dissolved oxygen data. The manuscript benefits from careful reading and constructive comments by James T. Hollibaugh. N. Jiao was supported by MOST (2007CB815900), NSFC (40632013 and 40821063), and SOA (200805068). C. Zhang was supported by NSFC (91028005) and the State Key Laboratory of Marine Geology Lecturer Professorship at Tongji University. A. Hu was supported by the MEL Young Scientist Visiting Fellowship (MELRS1026) from the State Key Laboratory of Marine Environmental Science at Xiamen University.

References

- Agogué H, Brink M, Dinasquet J, Herndl GJ (2008) Major gradients in putatively nitrifying and non-nitrifying archaea in the deep North Atlantic. *Nature* 456:788–791
- Aristegui J, Gasol JM, Duarte CM, Herndl GJ (2009) Microbial oceanography of the dark ocean’s pelagic realm. *Limnol Oceanogr* 54:1501–1529
- Auguet JC, Borrego CM, Baneras L, Casamayor EO (2008) Fingerprinting the genetic diversity of the biotin carboxylase gene (*accC*) in aquatic ecosystems as a potential marker for studies of carbon dioxide assimilation in the dark. *Environ Microbiol* 10:2527–2536
- Bano N, Ruffin S, Ransom B, Hollibaugh JT (2004) Phylogenetic composition of Arctic Ocean archaeal assemblages and comparison with Antarctic assemblages. *Appl Environ Microbiol* 70:781–789
- Beman JM, Roberts KJ, Wegley L, Rohwer F, Francis CA (2007) Distribution and diversity of archaeal ammonia monooxygenase genes associated with corals. *Appl Environ Microbiol* 73:5642–5647
- Beman JM, Popp BN, Francis CA (2008) Molecular and biogeochemical evidence for ammonia oxidation by marine Crenarchaeota in the Gulf of California. *ISME J* 2:429–441
- Beman JM, Sachdeva R, Fuhrman JA (2010) Population ecology of nitrifying archaea and bacteria in the Southern California Bight. *Environ Microbiol* 12:1282–1292
- Berg IA, Kockelkorn D, Buckel W, Fuchs G (2007) A 3-hydroxypropionate/4-hydroxybutyrate autotrophic carbon dioxide assimilation pathway in archaea. *Science* 318:1782–1786
- Brochier-Armanet C, Boussau B, Gribaldo S, Forterre P (2008) Mesophilic Crenarchaeota: proposal for a third archaeal phylum, the Thaumarchaeota. *Nat Rev Microbiol* 6:245–252
- Carpenter JH (1965) The Chesapeake Bay Institute technique for the Winkler dissolved oxygen method. *Limnol Oceanogr* 10:141–143
- Chen CTA, Wang SL, Wang BJ, Pai SC (2001) Nutrient budgets for the South China Sea basin. *Mar Chem* 75:281–300
- Church MJ, Wai B, Karl DM, DeLong EF (2010) Abundances of crenarchaeal *amoA* genes and transcripts in the Pacific Ocean. *Environ Microbiol* 12:679–688
- Crump BC, Baross JA (2000) Archaeoplankton in the Columbia River, its estuary and the adjacent coastal ocean, USA. *FEMS Microbiol Ecol* 31:231–239
- Dang H, Li J, Zhang X, Li T, Tian F, Jin W (2009) Diversity and spatial distribution of *amoA*-encoding archaea in the deep-sea sediments of the tropical West Pacific Continental Margin. *J Appl Microbiol* 106:1482–1493
- Dang H, Luan XW, Chen R, Zhang X, Guo L, Klotz MG (2010) Diversity, abundance and distribution of *amoA*-encoding archaea in deep-sea methane seep sediments of the Okhotsk Sea. *FEMS Microbiol Ecol* 72:370–385
- De Corte D, Yokokawa T, Varela MM, Agogue H, Herndl GJ (2009) Spatial distribution of bacteria and archaea and *amoA* gene copy numbers throughout the water column of the Eastern Mediterranean Sea. *ISME J* 3:147–158
- de la Torre JR, Walker CB, Ingalls AE, Konneke M, Stahl DA (2008) Cultivation of a thermophilic ammonia oxidizing archaeon synthesizing crenarchaeol. *Environ Microbiol* 10:810–818
- DeLong EF (1992) Archaea in coastal marine environment. *Proc Natl Acad Sci USA* 89:5685–5689
- DeLong EF, Wu KY, Prhelin BB, Jovine RV (1994) High abundance of archaea in Antarctic marine picoplankton. *Nature* 371:695–697
- Ettema TJG, Andersson SGE (2008) Comment on “A 3-hydroxypropionate/4-hydroxybutyrate autotrophic carbon dioxide assimilation pathway in archaea”. *Science* 321:342b
- Falster DS, Warton DI, Wright IJ (2006) SMATR: Standardised major axis tests and routines, ver 2.0. Available at: <http://www.bio.mq.edu.au/ecology/SMATR>
- Francis CA, Roberts KJ, Beman JM, Santoro AE, Oakley BB (2005) Ubiquity and diversity of ammonia-oxidizing archaea in water columns and sediments of the ocean. *Proc Natl Acad Sci USA* 102:14683–14688
- Fuhrman JA, McCallum K, Davis AA (1992) Novel major archaeobacterial group from marine plankton. *Nature* 356:148–149
- Fuhrman JA, Davis AA (1997) Widespread archaea and novel bacteria from the deep sea as shown by 16S rRNA gene sequences. *Mar Ecol Prog Ser* 150:275–285
- Galand PE, Lovejoy C, Hamilton AK, Ingram RG, Pedneault E, Carmack EC (2009) Archaeal diversity and a gene for ammonia oxidation are coupled to oceanic circulation. *Environ Microbiol* 11:971–980
- García-Martínez J, Rodríguez-Valera F (2000) Microdiversity of uncultured marine prokaryotes: the SAR11 cluster and the marine archaea of group I. *Mol Ecol* 9:935–948
- Good IJ (1953) The population frequencies of species and the estimation of population parameters. *Biometrika* 40:237–264
- Hallam SJ, Mincer TJ, Schleper C, Preston CM, Roberts K, Richardson PM, DeLong EF (2006) Pathways of carbon assimilation and ammonia oxidation suggested by environmental genomic analyses of marine Crenarchaeota. *PLoS Biol* 4:e95
- Hansman RL, Griffin S, Watson JT, Druffel ERM, Ingalls AE, Pearson A, Aluwihare LI (2009) The radiocarbon signature of microorganisms in the mesopelagic ocean. *Proc Natl Acad Sci USA* 106:6513–6518
- Herfort L, Schouten S, Abbas B, Veldhuis MJW, Coolen MJL, Wuchter C, Boon JP, Herndl GJ, Damste JSS (2007) Variations in

- spatial and temporal distribution of archaea in the North Sea in relation to environmental variables. *FEMS Microbiol Ecol* 62:242–257
31. Herndl GJ, Reinthaler T, Teira E, van Aken H, Veth C, Pernthaler A, Pernthaler J (2005) Contribution of Archaea to total prokaryotic production in the deep Atlantic Ocean. *Appl Environ Microbiol* 71:2303–2309
 32. Hu A, Yao T, Jiao N, Liu Y, Yang Z, Liu X (2010) Community structures of ammonia-oxidizing archaea and bacteria in high-altitude lakes on the Tibetan Plateau. *Freshwat Biol* 55:2375–2390
 33. Ingalls AE, Shah SR, Hansman RL, Aluwihare LI, Santos GM, Druffel ERM, Pearson A (2006) Quantifying archaeal community autotrophy in the mesopelagic ocean using natural radiocarbon. *Proc Natl Acad Sci USA* 103:6442–6447
 34. Jia ZJ, Conrad R (2009) Bacteria rather than Archaea dominate microbial ammonia oxidation in an agricultural soil. *Environ Microbiol* 11:1658–1671
 35. Könneke M, Bernhard AE, de la Torre JR, Walker CB, Waterbury JB, Stahl DA (2005) Isolation of an autotrophic ammonia-oxidizing marine archaeon. *Nature* 437:543–546
 36. Kalanetra KM, Bano N, Hollibaugh JT (2009) Ammonia-oxidizing archaea in the Arctic Ocean and Antarctic coastal waters. *Environ Microbiol* 11:2434–2445
 37. Kamer MB, DeLong EF, Karl DM (2001) Archaeal dominance in the mesopelagic zone of the Pacific Ocean. *Nature* 409:507–510
 38. Konstantinidis KT, Braff J, Karl DM, DeLong EF (2009) Comparative metagenomic analysis of a microbial community from 4000 m at Station ALOHA in the North Pacific Subtropical Gyre. *Appl Environ Microbiol* 75:5345–5355
 39. Kowalchuk GA, Stephen JR (2001) Ammonia-oxidizing bacteria: a model for molecular microbial ecology. *Annu Rev Microbiol* 55:485–529
 40. López-García P, Moreira D, López-Lopez A, Rodriguez-Valera F (2001) A novel haloarchaeal-related lineage is widely distributed in deep oceanic regions. *Environ Microbiol* 3:72–78
 41. La Cono V, Smedile F, Ferrer M, Golyskin PN, Giuliano L, Yakimov MM (2010) Genomic signatures of fifth autotrophic carbon assimilation pathway in bathypelagic Crenarchaeota. *Microb Biotechnol* 3:595–606
 42. Leininger S, Urich T, Schloter M, Schwark L, Qi J, Nicol GW, Prosser JI, Schuster SC, Schleper C (2006) Archaea predominate among ammonia-oxidizing prokaryotes in soils. *Nature* 442:806–809
 43. Liu B, Ye GB, Wang FP, Bell R, Noakes J, Short T, Zhang CL (2009) Community structure of archaea in the water column above gas hydrates in the Gulf of Mexico. *Geomicrobiol J* 26:363–369
 44. Ludwig W, Strunk O, Westram R, Richter L, Meier H, Yadhukumar BA, Lai T, Steppi S, Jobb G, Forster W, Brettske I, Gerber S, Ginhart AW, Gross O, Grumann S, Hermann S, Jost R, König A, Liss T, Lussmann R, May M, Nonhoff B, Reichel B, Strehlow R, Stamatakis A, Stuckmann N, Vilbig A, Lenke M, Ludwig T, Bode A, Schleifer KH (2004) ARB: a software environment for sequence data. *Nucleic Acids Res* 32:1363–1371
 45. Magalhaes CM, Machado A, Bordalo AA (2009) Temporal variability in the abundance of ammonia-oxidizing bacteria vs. archaea in sandy sediments of the Douro River estuary, Portugal. *Aquat Microb Ecol* 56:13–23
 46. Massana R, DeLong EF, Pedros-Alio C (2000) A few cosmopolitan phylotypes dominate planktonic archaeal assemblages in widely different oceanic provinces. *Appl Environ Microbiol* 66:1777–1787
 47. Mincer TJ, Church MJ, Taylor LT, Preston C, Karl DM, DeLong EF (2007) Quantitative distribution of presumptive archaeal and bacterial nitrifiers in Monterey Bay and the North Pacific Subtropical Gyre. *Environ Microbiol* 9:1162–1175
 48. Nakagawa T, Mori K, Kato C, Takahashi R, Tokuyama T (2007) Distribution of cold-adapted ammonia-oxidizing microorganisms in the deep-ocean of the northeastern Japan Sea. *Microbes Environ* 22:365–372
 49. Nicol GW, Tscherko D, Embley TM, Prosser JI (2005) Primary succession of soil Crenarchaeota across a receding glacier foreland. *Environ Microbiol* 7:337–347
 50. Nicol GW, Leininger S, Schleper C, Prosser JI (2008) The influence of soil pH on the diversity, abundance and transcriptional activity of ammonia oxidizing archaea and bacteria. *Environ Microbiol* 10:2966–2978
 51. Øvreås L, Forney L, Daae FL, Torsvik V (1997) Distribution of bacterioplankton in meromictic Lake Saelenvannet, as determined by denaturing gradient gel electrophoresis of PCR-amplified gene fragments coding for 16S rRNA. *Appl Environ Microbiol* 63:3367–3373
 52. Park BJ, Park SJ, Yoon DN, Schouten S, Damste JSS, Rhee SK (2010) Cultivation of autotrophic ammonia-oxidizing archaea from marine sediments in coculture with sulfur-oxidizing bacteria. *Appl Environ Microbiol* 76:7575–7587
 53. Purkhold U, Pommerening-Roser A, Juretschko S, Schmid MC, Koops HP, Wagner M (2000) Phylogeny of all recognized species of ammonia oxidizers based on comparative 16S rRNA and amoA sequence analysis: Implications for molecular diversity surveys. *Appl Environ Microbiol* 66:5368–5382
 54. Reinthaler T, van Aken HM, Herndl GJ (2010) Major contribution of autotrophy to microbial carbon cycling in the deep North Atlantic's interior. *Deep-Sea Res Pt II* 57:1572–1580
 55. Ronquist F, Huelsenbeck JP (2003) MrBayes 3: Bayesian phylogenetic inference under mixed models. *Bioinformatics* 19:1572–1574
 56. Rothauwe JH, Witzel KP, Liesack W (1997) The ammonia monooxygenase structural gene amoA as a functional marker: molecular fine-scale analysis of natural ammonia-oxidizing populations. *Appl Environ Microbiol* 63:4704–4712
 57. Santoro AE, Casciotti KL, Francis CA (2010) Activity, abundance and diversity of nitrifying archaea and bacteria in the central California current. *Environ Microbiol* 12:1989–2006
 58. Schleper C, Jurgens G, Jonuscheit M (2005) Genomic studies of uncultivated archaea. *Nat Rev Microbiol* 3:479–488
 59. Schloss PD, Handelsman J (2005) Introducing DOTUR, a computer program for defining operational taxonomic units and estimating species richness. *Appl Environ Microbiol* 71:1501–1506
 60. Schloss PD, Handelsman J (2006) Introducing SONS, a tool for operational taxonomic unit-based comparisons of microbial community memberships and structures. *Appl Environ Microbiol* 72:6773–6779
 61. Shaw PT, Chao SY, Liu KK, Pai SC, Liu CT (1996) Winter upwelling off Luzon in the north-eastern South China Sea. *J Geophys Res* 101:16435–16488
 62. Stahl DA, Amann R (1991) Development and application of nucleic acid probes. In: Stackebrandt E, Goodfellow M (eds) *Nucleic acid techniques in bacterial systematics*, vol 8, Wiley, Chichester, England, pp 205–248
 63. Spang A, Hatzepichler R, Brochier-Armanet C, Rattei T, Tischler P, Spieck E, Streit W, Stahl DA, Wagner M, Schleper C (2010) Distinct gene set in two different lineages of ammonia-oxidizing archaea supports the phylum Thaumarchaeota. *Trends Microbiol* 18:331–340
 64. Swofford DL (2003) PAUP*, phylogenetic analysis using parsimony (*and other methods), version 4. Sinauer Associates, Sunderland
 65. Treusch AH, Leininger S, Kletzin A, Schuster SC, Klenk HP, Schleper C (2005) Novel genes for nitrite reductase and Amo-related proteins indicate a role of uncultivated mesophilic

- crenarchaeota in nitrogen cycling. *Environ Microbiol* 7:1985–1995
66. Venter JC, Remington K, Heidelberg JF, Halpern AL, Rusch D, Eisen JA, Wu DY, Paulsen I, Nelson KE, Nelson W, Fouts DE, Levy S, Knap AH, Lomas MW, Nealson K, White O, Peterson J, Hoffman J, Parsons R, Baden-Tillson H, Pfannkoch C, Rogers YH, Smith HO (2004) Environmental genome shotgun sequencing of the Sargasso Sea. *Science* 304:66–74
 67. Walker CB, de la Torre JR, Klotz MG, Urakawa H, Pinel N, Arp DJ, Brochier-Armanet C, Chain PSG, Chan PP, Gollabgir A (2010) *Nitrosopumilus maritimus* genome reveals unique mechanisms for nitrification and autotrophy in globally distributed marine crenarchaea. *Proc Natl Acad Sci USA* 107:8818–8823
 68. Warton DI, Wright IJ, Falster DS, Westoby M (2006) Bivariate line-fitting methods for allometry. *Biol Rev* 81:259–291
 69. Wong GTF, Ku TL, Mulholland M, Tseng CM, Wang DP (2007) The SouthEast Asian time-series study (SEATS) and the biogeochemistry of the South China Sea—an overview. *Deep-Sea Res Pt II* 54:1434–1447
 70. Wuchter C, Abbas B, Coolen MJL, Herfort L, van Bleijswijk J, Timmers P, Strous M, Teira E, Herndl GJ, Middelburg JJ, Schouten S, Damsté JSS (2006) Archaeal nitrification in the ocean. *Proc Natl Acad Sci USA* 103:12317–12322
 71. Yakimov MM, La Cono V, Denaro R, D'Auria G, Decembrini F, Timmis KN, Golyshin PN, Giuliano L (2007) Primary producing prokaryotic communities of brine, interface and seawater above the halocline of deep anoxic lake L'Atalante, Eastern Mediterranean Sea. *ISME J* 1:743–755
 72. Yakimov MM, Conoa VL, Denaro R (2009) A first insight into the occurrence and expression of functional *amoA* and *accA* genes of autotrophic and ammonia-oxidizing bathypelagic Crenarchaeota of Tyrrhenian Sea. *Deep-Sea Res Pt II* 56:748–754
 73. Yakimov MM, La Cono V, Smedile F, DeLuca TH, Juarez S, Ciordia S, Fernandez M, Albar JP, Ferrer M, Golyshin PN, Giuliano L (2011) Contribution of crenarchaeal autotrophic ammonia oxidizers to the dark primary production in Tyrrhenian deep waters (Central Mediterranean Sea). *ISME J*. doi:10.1038/ismej.2010.1197
 74. Zhang M (2009) Productivity and nutrient dynamics in the modern South China Sea. In: Wang P, Li Q (eds) *The South China Sea. Paleooceanography and sedimentology*. Springer, New York, pp 439–457
 75. Zhang Y, Sintès E, Chen MN, Zhang Y, Dai MH, Jiao NZ, Herndl GJ (2009) Role of mesoscale cyclonic eddies in the distribution and activity of archaea and bacteria in the South China Sea. *Aquat Microb Ecol* 56:65–79